# AERODYNAMIC OPTIMIZATION AND BOUNDARY LAYER CONTROL ON SAILPLANE WING SECTIONS

L. Popelka, M. Matejka, N. Souckova
Academy of Sciences of the Czech Republic, Institute of Thermomechanics
Dolejskova 5, CZ 182 00 Prague
Czech Technical University in Prague, Faculty of Mechanical Engineering
Technicka 4, 166 07 Prague
Czech Republic

## OVERVIEW

Numerical analysis tools have been thoroughly verified and coupled with findings of wind-tunnel and flight evaluations. Optimization procedure has been used for multicriteria sailplane airfoil design with using of fitness function. Surface visualization has been carried out and separation regions along the wingspan studied on wings of two club class sailplanes. Passive flow control has been consequently applied at optimum location. Glide ratio has been measured and significant performance improvement has been gained.

## 1. INTRODUCTION

Initial design stage of every aircraft forms pronounced need of agile and reliable analysis methods implemented in optimization process, capable of modeling the main features of flow control. Wind-tunnel measurement can offer majority of required data, but applying cost effective numerical methods and coupling with in-flight findings are of paramount importance.

## 2. NUMERICAL METHODS

Finite-volume approach based on Reynolds Averaged Navier-Stokes and coupling of panel method with boundary layer equations were used in form of standard software packages Fluent and Xfoil. Both were thoroughly verified mainly for the purposes of aerodynamic coefficient calculations and range of usage with setting parameters was established.

### 2.1. Xfoil verification for low-turbulence-intensity free stream

Xfoil code [1] is considered as a standard tool for subsonic airfoil analysis. Cases for calculation of integral characteristics with natural and controlled transition have been verified. Although standard setting offer reasonable accuracy, significant shift have emerged with passive flow control, while compared to reliable experimental data.
For primary assessment NACA 6-series, altering the thickness distribution from 63-415 to 66-415 and also the family of Wortmann airfoils FX 63-145/158/147/143 have been used.
At given lift coefficient $c_L$, appropriate capture of differences should be proven between investigated (denoted i ) and reference ( ref ) airfoil, merely than absolute values of drag coefficient $c_D$. Following ratio can be defined:

$$f_{cD} = \frac{c_{Dref}}{c_{Di}} \tag{1}$$

Same approach can be used for both numerical ( num ) and experimental ( exp ) data. Principal objective is $f_{cD\,exp} / f_{cDnum} = 1$. Sufficient amount of proven wind tunnel data, concerning modern laminar airfoils, are available for comparison, originating from Laminarwindkanal of the TU Stuttgart (LWK), [2], [3] .
NACA 63-618, Wortmann FX66-S-196 and Eppler E603 airfoils have been further considered, with reference Wortmann FX61-163. Values of ratio according to equation (1) have been obtained, varying the n-factor in $e^n$ transition criteria, for values of Reynolds number Re = $10^6$, Tab. 1. Agreement with n = 9 is acceptable for the given purpose.

| | $f_{cD\,exp\,LWK} / f_{cDnumXfoil}$ | |
|---|---|---|
| n | free transition (FX61-163, FX66-S-196, E603, NACA63-618) | controlled transition (AH82-150F, 4 combinations of turbulators) |
| 5 | 0.979 ± 0.030 | 1.047 ± 0.024 |
| 9 | 0.992 ± 0.015 | 0.906 ± 0.020 |
| 11 | 1.007 ± 0.022 | 0.837 ± 0.031 |

Tab. 1 Agreement between experimental and calculated $c_D$ values, range $c_L$ = 0.2 ÷ 0.9, confidence 95%

Airfoil Althaus AH82-150F, designed for flow control on both sides offers second suitable test case. All four possibilities – clean airfoil, upper and lower turbulators installed and both of them simultaneously – have been examined at Re = 106, Tab. 1. Although agreement with n = 9 is again found to be acceptable, mean value of $f_{cDnumXfoil}$ is shifted against $f_{cD\,exp\,LWK}$. There is apparent over-estimation of performance gains due to transition control in numerical calculation. Hence adequate care should be taken in such analysis and further need to research the influence of transition control to the separation bubble have been justified.

Higher level of free stream turbulence, which is observed within thermals and hence met by sailplane in flight, have been modelled by simple relation between turbulence intensity Tu and n-factor (as proposed by Mack (1977) and implemented in Xfoil code).

Fluent software have been used to simulate effect of roughness due to insect on airfoil drag properties, by modeling fully turbulent boundary layer. Calculated fields of velocity magnitude and static pressure, e.g. Fig. 1, were also employed in feasibility studies of experimental programme.

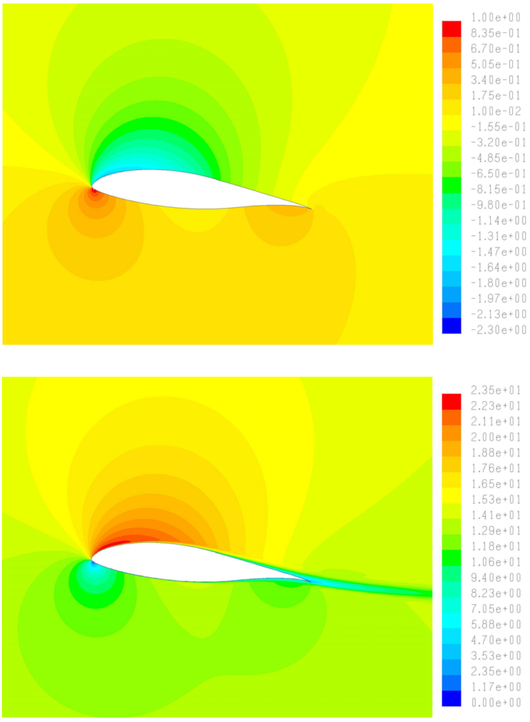

Fig. 1 Calculated pressure-coefficient $c_P$ field (upper) and velocity magnitude V [m/s] (lower), airfoil Wortmann FX61-163, Fluent 6.0, Spalart-Almaras turbulence model

## 3. EXPERIMENTAL METHODS

In order to acquire parameters which cannot be obtained by numerical modeling, to prove calculated data and also to receive more insight into transition, separation and their control, both wind-tunnel and in-flight testing methods were applied.

### 3.1. Wind-tunnel testing

Two wind tunnels of the Czech Technical University, 750x550mm and 1200x400mm, and blown-down rig 250x250mm of the Academy Sciences were used.

### 3.1.1. Visualization

Smoke-wire visualization have been carried out on lower free stream Reynolds numbers than correspond to free flight with aim to demonstrate laminar separation, transition completion in free shear layer and turbulent reattachment in more pronounced manner, Fig. 2. Reference Wortmann airfoil FX66-17AII-182 and two new designs, PW212-163, PW311-161, [4], have been used. In comparison with reference airfoil, smaller extent of separation have been observed, as well as higher portion of laminar boundary layer.

Visualization techniques have been also used in optimization of passive transition control. Zig-zag tape have been applied on lower surfaces of the PW212-163 and PW311-161 airfoils and sequence of digital images acquired.

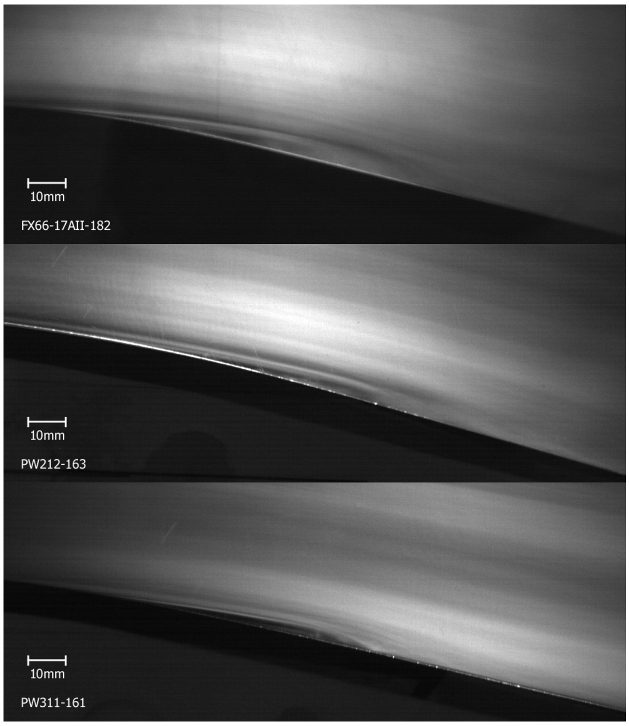


Fig. 2 Smoke-wire visualization, airfoils FX66-17AII-182, PW212-163, PW311-161, $\alpha$ = 0deg, Re = 1.7 $10^5$

### 3.1.2. Integral data

Since maximum lift coefficient cannot be reasonably predicted by methods mentioned in section 2, measurement of lift curve of three airfoil mentioned in section 3.1.1. was performed, Fig. 3. The blown-down rig 250x250mm was used to check the functionality of new drag rake designed for in-flight measurement.

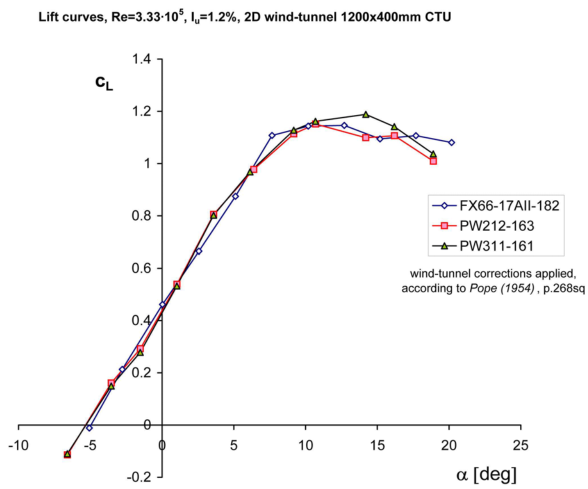


Fig. 3 Measured lift curves of reference and examined airfoils in 1200x400mm 2D wind-tunnel.

## 3.2. In-flight testing

Testing programme was accomplished on two club class sailplanes, Standard Cirrus and TST-10M Atlas. Surface oil-flow for separation bubble visualization and tufts for stalled region in the wing-fuselage transition was used. Speed-polar measurements were executed by GNSS devices and improvement by flow-control assessed. Performance gains were reached and both test sailplanes flown on top competitions.

### 3.2.1. Visualization

Thin film of oil have revealed separated regions along the wingspan of both studied sailplanes, Fig 4. Agreement between measured and calculated location has been found very good. CFD and wind-tunnel data of corresponding wing section have been also used for application of flow control.

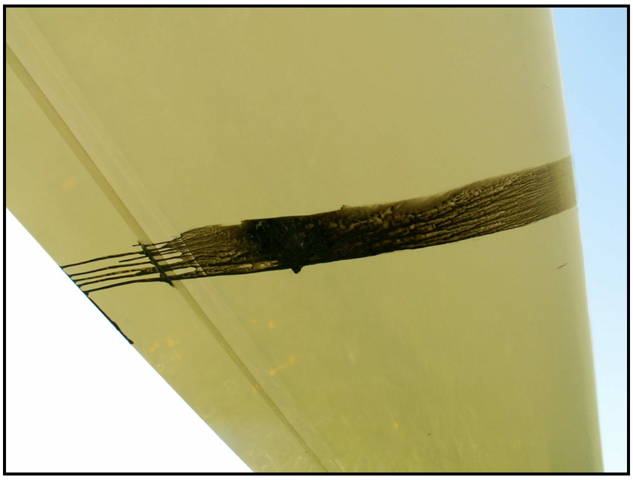

Fig. 4 Oil-flow visualization on lower surface of outer wing segment of TST-10M sailplane, in the aileron region. V = 100 km/h IAS. Right to left: laminar boundary layer, separation bubble, turbulent boundary layer

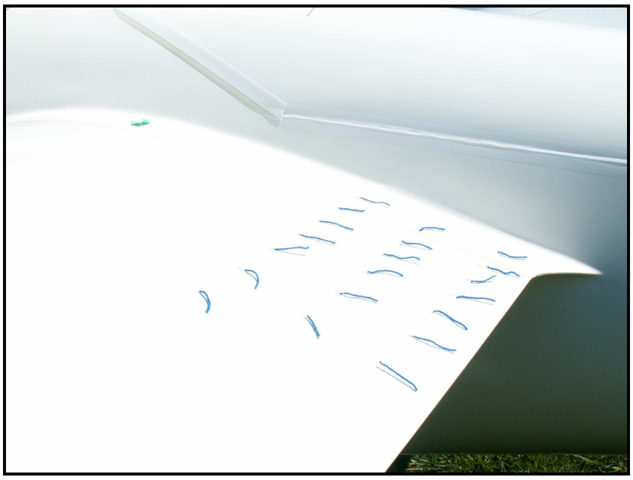

Fig. 5 Array of tufts and vortex generator installed on the left wing root of TST-10M prior to the test flight

Based on previous investigations on TST-10M sailplane, visualization in the transition wing-fuselage geometry have been done by tufts, Fig 5, on four airspeeds covering the common competition range. Region of separated flow have been determined, vortex generator applied and separation suppression observed. Effect on performance of sailplane have been consequently confirmed by measuring both uncontrolled and controlled speed polar of the test sailplane.

### 3.2.2. Performance measurement

Flow visualization have revealed regions of separated flow. Passive devices have been applied in form of Zig-zag tape and counter-rotating vortex generators.

GNSS devices LX7007 and LX20 were used to acquire GPS signal, which was post-processed and reduced to International Standard Atmosphere. Measured improvements of glide ratio L/D of the Standard Cirrus by transition control are summarized in Tab. 2

| V [km/h] IAS | Δ L/D | Δ L/D [%] |
|---|---|---|
| 115 | 3 | 10,7 |
| 140 | 2 | 7,7 |

Tab. 2 Measured glide ratio of Standard Cirrus sailplane and effect of separation bubble suppression

At the 85 km/h IAS, improvement of 1.7 L/D have been gained on TST-10M sailplane by vortex generators.

The Standard Cirrus SN 385, OK-7077 /CX/ was flown by Mr. Petr Krejcirik on 4$^{th}$ Club Class World Gliding Championship 2006, 3$^{rd}$ overall position reached. TST-10M OK-A631 /LZ/ was prepared for Czech National Soaring Championship 2007 to be flown by Mr. Lubor Zeleny.

## 4. SYNTHESIS AND OPTIMIZATION

Methods of numerical and experimental analysis presented in previous sections were coupled together to obtain value of fitness function of examined airfoil with comparison to the reference one. Inviscid pressure distribution was modified and inverse method used to generate new airfoil geometry, simplex optimization method applied to maximize the fitness function within given constraints. Aerodynamic criteria, based on a questionnaire survey, [5], were used.

## 5. RESULTS

Optimization procedure has been used for 4 different set of constraints – sailplane class, airfoil chord and thickness and 4 new airfoils developed, Fig. 6. Referring to Wortmann FX66-17AII-182, with F=100%, following values of fitness function have been obtained: PW211-196, F=105,5%; PW212-163, F=110,7%; PW311-161, F=108,7%; PW312-161, F=106,4%.

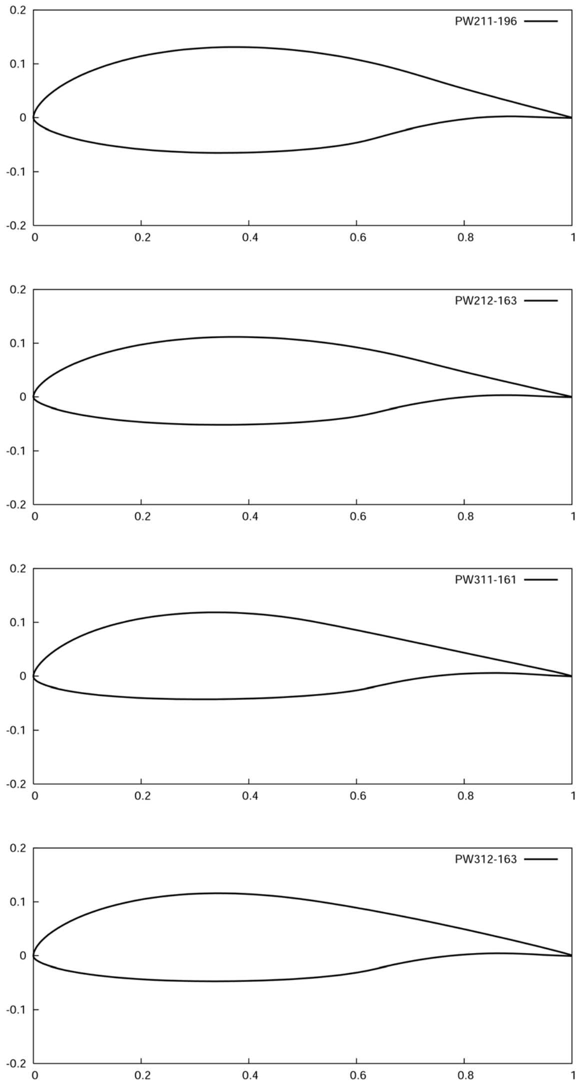


Fig. 6 Geometry of PW series airfoils, 2xx for root and 3xx for tip wing section

Furthermore, the possibility of adaptive control has been studied on flapped airfoil, Fig. 7, [6]. Prediction of Xfoil solution shows markedly different locations of laminar separation and hence need for action with feedback to the instantaneous conditions in the boundary layer.

Whether drag reduction while positive flap deflection can be materialized, remains to be investigated. For such purposes, drag rake has been prepared and in-flight tests are under preparation.

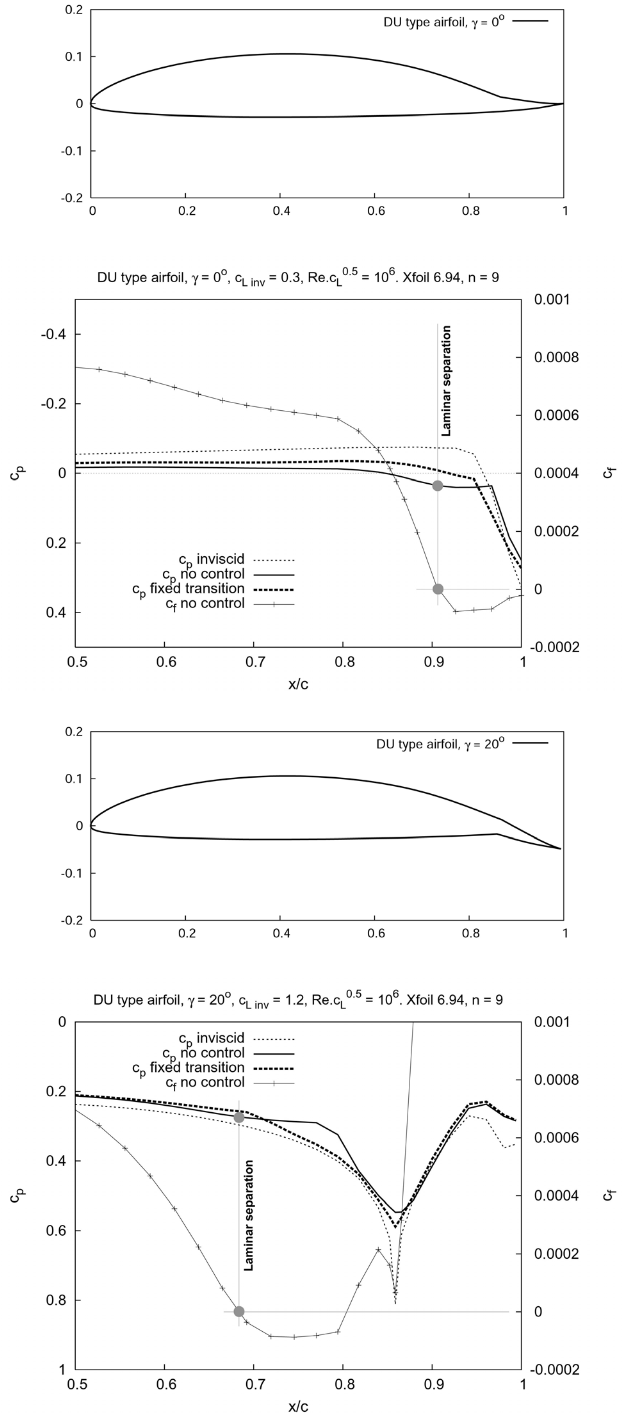


Fig. 7 Geometry of flapped airfoil for flap deflection $\gamma = 0$ deg and $\gamma = 20$ deg respectively, calculated pressure distributions $c_P$ and skin friction coefficient $c_f$ on lower surface. Location of laminar separation onset for case without boundary layer control

## 6. LITERATURE

[1] Drela, M., Youngren, H.: Xfoil 6.9 User Guide. MIT, 2001, 33 p., URL: http://raphael.mit.edu/xfoil/

[2] Althaus, D., Wortmann, F.X.: Stuttgarter Profilkatalog I. 1st Ed. Braunschweig: Vieweg & Sohn Verlagsgesellschaft, 1981. 319 p. ISBN 3-528-08464-2

[3] Althaus, D.: Niedriggeschwindigkeitsprofile. 1st Ed. Braunschweig: Vieweg & Sohn Verlagsgesellschaft, 1996. 592 p. ISBN 3-528-03820-9

[4] Popelka, L.: PW series airfoils - numerical optimization and wind-tunnel measurement. In. Colloquium Fluid Dynamics. Prague: Institute of Thermomechanics AS CR, 2005, p. 117-120

[5] Popelka, L., Matejka, M.: Optimization Criteria and Sailplane Airfoil Design. In. Technical Soaring, Vol. 30 (2006), No. 3, p. 74-78. ISSN 07448996

[6] Matejka, M., Popelka, L.: The Study of Influence of Active and Passive Methods of Boundary Layer Control. Presented at the XXVIII OSTIV Congress, Eskilstuna, Sweden, 8 – 15 June 2006. In the review process for publishing in Technical Soaring

## 7. ACKNOWLEDGMENT

Authors would like to express their thanks to Mr. Lubor Zeleny, who have piloted all test flights with sailplane TST-10M and to Mr. Petr Krejcirik, who have carried out the programme on Standard Cirrus.

The work has been supported by the Ministry of Education, Youth and Sports of the Czech Republic, within project No. 1M06031.

Also grant support of GA AS CR No. IAA2076403, No. IAA200760614 is gratefully acknowledged.